CORE
Metadata, citation and similar papers at core.ac.uk
Provided by Elsevier - Publisher Connector



knees but have significant underlying skeletal defects including thinner bones that spontaneously fracture. The purpose of this study was to define the role of BMP2 in the formation and maintenance of the knee joint. In order to do this, we removed BMP2 specifically from synovial joint cells using the Gdf5-cre transgene.
**Methods:** We generated BMP2 loss of function conditional mutant mice using BMP2 floxed alleles. The Gdf5-cre transgene was used to specifically delete BMP2 within synovial joints (BMP2-Gdf5 cKO) starting at embryonic day 12.5 (E12.5). We performed histology, immunohistochemistry (IHC), qRT-PCR, Xradia micro-CT, and Atomic Force Microscopy based (AFM) nanoindentation to assess both molecular and biomechanical changes in articular cartilage and meniscus during joint formation, maturation and maintenance using hindlimbs isolated from E17, 2 week, 8-10 week and 5 month old mice.
**Results:** Loss of BMP2 from synovial joint forming cells (BMP2-Gdf5 cKO) does not affect knee joint morphogenesis. At E17, the developing meniscus, ligaments and articular surfaces of the tibia and femur all appeared normal. At 2 weeks after birth, when joint structures are maturing, the meniscus of the BMP2-Gdf5 cKO knees appeared developmentally delayed when compared to controls. Saf-O staining showed reduced proteoglycan expression as well as decreased rounded chondrocyte like cells in BMP2-Gdf5 cKO meniscus. IHC analysis revealed reduced collagen type 2 (Col2) and altered aggrecan distribution in BMP2-Gdf5 cKO meniscus while picrosirius red staining showed a disorganized pattern of collagen fibers. This data was confirmed using qPCR analysis that showed a decrease in both Col2 and aggrecan expression in 2 wk old menisci from BMP2-Gdf5 cKO mice compared to controls and revealed that BMP target genes Lox (lysl oxidase) and Runx2 were also down regulated. AFM nanoindentation testing of knee joints of 2 wk old BMP2-Gdf5 and control mice revealed no significant differences in the nanomechanical properties of the articular cartilages. However, menisci from BMP2-Gdf5 KO mice appeared to have weakened mechanical function with significantly lower indentation stiffness when compared to controls. By 8-10 weeks of age, menisci from BMP2-Gdf5 cKO knees appeared to be less ossified and continued to have decreased expression of ECM components. In addition, knee joints of the BMP2-Gdf5 cKO mice started to show signs of early OA as the articular cartilage began to fibrillate. By 5 months of age, Xradia micro-CT analysis showed loss of BMP2 results in joint space narrowing, flattened tibial epiphyses, menisci that are smaller and significantly less well mineralized, but no evidence of osteophyte formation. IHC analysis of 5 month old BMP2-Gdf5 cKO knees revealed distinct signs of progressive OA pathology including decreased expression of Col2, aggrecan and pSmad2 and increased expression of collagen type X (ColX) and ADAMTS5 when compared to controls.
**Conclusions:** BMP signaling provided by BMP2 is not required for knee joint formation during development but is necessary for the maintenance of knee joint function after birth. Our findings reveal an important role for BMP2 in the proper assembly and maturation of the meniscus ECM that appears to be essential for joint homeostasis as mice lacking BMP2 in Gdf5 + cells develop spontaneous OA as they age. Our data point to an important role for BMP2 production by cells in the knee joint and suggest that interventions that allow for the maintenance of adequate local BMP2 expression by these structures may be of benefit in the prevention of age related knee OA.

## 56
## E11 PROTEIN STABILISATION BY PROTEASOME INHIBITION PROMOTES OSTEOCYTE DIFFERENTIATION AND MAY PROTECT AGAINST OSTEOARTHRITIS BONE PATHOLOGY

K.A. Staines †, M. Prideaux ‡, P. Hohenstein †, D.J. Buttle §, A.A. Pitsillides ‖, C. Farquharson †. † *Roslin Inst., Univ. of Edinburgh, Edinburgh, Midlothian, United Kingdom;* ‡ *Univ. of Adelaide, Adelaide, Australia;* § *Univ. of Sheffield, Sheffield, United Kingdom;* ‖ *Royal Vet. Coll., London, United Kingdom*

**Purpose:** The mechanisms which govern osteoblast-to-osteocyte transitions (osteocytogenesis) are yet to be established, however their dysregulation is likely to contribute to osteoarthritic (OA) subchondral bone sclerosis. The transmembrane glycoprotein E11 is critical in early osteocyte commitment thus here we sought to determine the mechanism regulating its expression during osteocytogenesis and to examine whether this was compromised in OA.
**Methods:** We have used immunohistochemistry, RT-qPCR and western blotting to examine the temporal and spatial localisation of E11 during osteocytogenesis. To examine the functional role of E11 we transfected the late osteoblast MLO-A5 cell line with E11 over-expressing and empty vector pLVX plasmids using Fugene HD. Using these cells we have investigated the post-translational regulation of E11, through addition of calpain and proteasome inhibitors (Z-FA-FMK, E64d, calpeptin, ALLN and MG132, lactacystin, Bortezomib, Withaferin-A, respectively) and subsequent western blotting and RT-qPCR analysis. We have generated mice harbouring a conditional deletion of E11 in late osteoblasts (osteocalcin promoter driven) (OB-E11-/-) and analysed its bone phenotype through histology, RT-qPCR and micro-CT scanning. We have also examined the natural OA model, the STR/Ort mouse, with regards to E11 expression.
**Results:** We reveal increased expression of E11 protein/mRNA ($P<0.001$) concomitant with extensive osteocyte dendrite formation and matrix mineralization ($P<0.001$) in MLO-A5 cell cultures. Whilst MLO-A5 cells transfected with E11 over-expressing pLVX plasmids exhibited significantly increased mRNA expression ($P<0.001$), western-blotting failed to detect any correlative increases in protein expression, suggestive of post-translational regulation. We therefore treated MLO-A5 cells with calpeptin and ALLN and found that both promoted E11 protein expression, with ALLN having the greatest effect. Treatment of MLO-A5 cells and osteocytic IDG-SW3 cells with ALLN also induced a profound increase in stellate cell morphology (50%, $P<0.001$) and increased E11 protein expression, whilst calpeptin treatment failed to promote similar osteocytogenic changes. Alternative calpain inhibitors E64d and Z-FA-FMK also failed to modify MLO-A5 cell morphology or E11 protein expression. Unchanging calpain 1/2 levels upon osteocytic differentiation during 15-day MLO-A5 time course suggests lack of calpain contribution to osteocytogenesis. Due to the dual roles for ALLN in calpain and proteasome inhibition, this characterized proteasomal degradation as the key pathway in E11 post-translational targeting and degradation. This was supported by studies using the proteasome inhibitors MG132, lactacystin, Bortezomib and Withaferin-A which produced similar dose-dependent increases in E11 expression in MLO-A5 cells. These data implicate proteasome degradation in controlling E11 stability. Preliminary microCT analyses of OB-E11-/- mice revealed decreased trabecular bone volume/tissue volume (27%) associated with decreased trabecular number (16%) and thickness (7%) in comparison to control mice. This pilot data has also revealed that the conditional deletion of E11 in osteoblasts results in decreased cortical cross-sectional thickness (12%). Further analyses will enable a more thorough skeletal phenotyping of these mice which will include osteocyte number and dendrite formation. Examination of a natural model of OA, the STR/Ort mouse, revealed decreased E11 protein expression in the subchondral bone osteocytes in regions of the joint where OA pathology is observed.
**Conclusions:** Together these data suggest that proteasome-mediated E11 protein degradation limits acquisition of the osteocyte phenotype and that its deregulation may contribute to bone changes observed in OA.

## 57
## PATHOGENESIS OF CAM MORPHOLOGY IN ENGLISH PREMIERSHIP FOOTBALLERS

A.J. Palmer †, S. Folkard †, M. Gimpel ‡, J. Broomfield †, J. Newton †, E. McNally †, A. Taylor †, K. Javaid †, A. Carr †, S. Glyn-Jones †. † *Univ. of Oxford, Oxford, United Kingdom;* ‡ *Southampton Football Club, Southampton, United Kingdom*

**Purpose:** Femoroacetabular impingement (FAI) is a cause of pain and osteoarthritis. The pathogenesis of this condition remains poorly understood and this limits the ability to develop treatment strategies. Cam morphology is thought to develop during adolescence, often in association with intense sporting activity. Postulated mechanisms include a subclinical slipped upper femoral epiphysis (SUFE) or extension of the epiphysis along the anterosuperior femoral neck. Cam morphology has an extremely high prevalence amongst professional footballers making them an ideal cohort to study disease pathogenesis.
**Methods:** Players at an English Premiership Football (Soccer) Club Academy were invited to participate using a randomisation algorithm within each age group. The cross-sectional cohort was loaded towards the youngest age groups to enhance a future longitudinal study. 20 players were selected from the U10 and U11 teams, and 10 players from the U12, U13, U14, U15, U16, and U18 teams (n=100).

Assessments were performed mid-season and included morphological MRI of both hips at 3T (in addition to a questionnaire, clinical examination, urine collection and physiological MRI). Morphological measurements were performed on 30 degree radial slices using Hipmorf software and included i) alpha angle measuring outline of bone ii) alpha angle measuring outline of cartilage iii) anterosuperior physeal extension (distance from medial femoral head to lateral extent of physis parallel with neck axis and divided by femoral head diameter) iv) metaphysis-neck offset (distance from metaphysis to outer border of femoral head perpendicular to neck axis and divided by femoral head diameter).

**Results:** Maximum alpha angle measured on all radial slices increased with age (bone alpha angle r = 0.47 p<0.0001, cartilage alpha angle r=0.63 p<0.0001) and was higher in players with any degree of physeal closure (mean 78.6 degrees) compared with players with an open physis (mean 64.0 degrees) (p<0.0001).

Alpha angle was highest at the 1 O'Clock position. Using a threshold of 60 degrees at this position, alpha angles were first raised for cartilage at 10 years of age and bone at 13 years of age. In the youngest age groups, raised cartilage alpha angles were secondary to hypertrophy of the outer border of the physis. Beyond 13 years of age, alpha angles were raised secondary to epiphyseal extension at the same site.

The prevalence of cam morphology in participants aged over 16 years of age was 75% for bone alpha angle (mean 73.3) and 82% for cartilage alpha angle (mean 77.3). Cam morphology was bilateral in 91% cases and there was no statistically significant difference in the alpha angle between left and right hips. Alpha angle correlated with anterosuperior epiphyseal extension (cartilage r=0.702 p<0.0001, bone r=0.500 p<0.0001) but not metaphysis-neck offset (cartilage r=0.040 p=0.569, bone r=0.041 p=0.564). Absolute offset increased linearly with age at every radial slice (r = 0.88 p<0.0001) and there was no evidence of SUFE.

**Conclusions:** Cartilaginous hypertrophy at the femoral head-neck junction precedes the appearance of an ossified cam lesion. This is consistent with findings from studies that show internal rotation is lost prior to radiographic evidence of FAI. Early morphological changes appear to represent the novel finding of hypertrophy at the groove of Ranvier and perichondral ring of LaCroix that is followed by epiphyseal migration along the anterosuperior femoral neck. It is this mechanism that gives rise to cam morphology within this cohort and not SUFE. We hypothesise that this represents a physiological response to loading and this is compatible with the bilateral nature of the condition. We have now finished recruitment of an age-matched local population control group that will give further insight into cam lesion development.

## 58
## HIP SHAPE BY STATISTICAL SHAPE MODELING IS ASSOCIATED WITH LEG LENGTH INEQUALITY IN OLDER ADULTS

Y.M. Golightly †, J.L. Stiller †, J. Cantrell †, J.B. Renner †, J.M. Jordan †, R.M. Aspden ‡, J.S. Gregory ‡, A.E. Nelson †. † *Univ. of North Carolina at Chapel Hill, Chapel Hill, NC, USA;* ‡ *Univ. of Aberdeen, Aberdeen, United Kingdom*

**Purpose:** Both leg length inequality (LLI) and altered hip shape are associated with hip osteoarthritis (OA), and these 2 risk factors may be related. Here we present the first exploration of the relationship between LLI and hip shape, accounting for radiographic hip OA.

**Methods:** Participants with knee or hip symptoms and suspected LLI identified from the Johnston County OA Project were invited to participate in a shoe lift intervention trial. Standing anteroposterior pelvic radiographs were obtained for each participant, the difference in height between the superior aspects of the femoral heads was measured by a trained reader, and LLI status (present: ≥1/8 inch difference between limbs) and the longer limb (right/left) were recorded. For 30 participants, another reader independently repeated these measures. A 77-point statistical shape model was used to define the shape of the proximal femur and adjacent pelvis on the radiographs. Shape software was used to generate scores representing independent modes of shape variation. Inter- and intra-reader repeatability for point placement was explored. Each hip was read using the Kellgren-Lawrence score (K-L) for the presence (K-L=2-4) or absence (K-L=0-1) of OA. Hip-based logistic regression models for 3 outcomes (Short limb vs. no LLI; Long limb vs. no LLI; Long vs. Short limb) were adjusted for age, sex, presence of hip OA, and intra-person correlation between hips.

**Results:** Of the 46 individuals (92 hips) enrolled in the clinical trial, 8 hips in 7 people were excluded (5 hip replacement, 3 unreadable films) leaving 45 people (mean age 70 ± 8 years, mean BMI 30 ± 3 kg/m2, 18% male, 27% African American) with 84 hips for shape analyses. Agreement between the 2 readers was 100% for LLI status and the longer limb. For point placement within 2 mm, intra- and inter-reader agreement were 100% and 92%, respectively. The first 11 modes explained >80% of the total shape variance. In adjusted models, alterations in modes 1 (figure), 8, and 10 were associated with hips from the shorter limbs of participants with LLI compared with participants without LLI (table). Although not statistically significant, variations in mode 3 were associated with hips from the shorter limbs of participants with LLI (adjusted odds ratio 3.33, 95% confidence interval 0.98, 11.28). Variations in modes 2, 6, 8, and 10 were associated with hips from the longer limb of LLI participants. A 1-SD increase in modes 1 and 6 at the hip were associated with 2.92 and 2.63 times the odds, respectively, of being from the longer versus the shorter limb in a participant with LLI, while an increase in mode 3 (figure) was associated with reduced odds of being from the longer limb.

**Conclusions:** Those with LLI show consistent variations in radiographic hip shape after controlling for hip OA and other key covariates. Prior work demonstrated associations between modes 2 and 3 with incident hip OA, and these modes, along with 6, 8, and 10, were linked to LLI. Although in this cross-sectional analysis we cannot determine causality, it is possible that the biomechanics of LLI led to hip remodeling or that hip shape led to LLI. Future work will clarify these associations and investigate potential predictive value of hip shape on response to LLI interventions.

Associations of 1-Standard Deviation Increase in Mode Score and Leg Length Inequality (LLI) Outcome

| Mode | % Variance | Short limb vs. no LLI | Long limb vs. no LLI | Long vs. short LLI limb |
|---|---|---|---|---|
| | (total 81%) | aOR (95% CI)* | aOR (95% CI) | aOR (95% CI) |
| 1 | 23.1 | 0.21 (0.07, 0.65) | 0.67 (0.22, 2.10) | 2.92 (1.45, 5.88) |
| 2 | 12.2 | 0.20 (0.01, 3.36) | 0.08 (0.02, 0.38) | 0.50 (0.17, 1.48) |
| 3 | 10.6 | 3.33 (0.98, 11.28) | 1.17 (0.44, 3.16) | 0.38 (0.19, 0.79) |
| 4 | 8.2 | 1.45 (0.59, 3.55) | 1.49 (0.60, 3.66) | 1.43 (0.63, 3.24) |
| 5 | 7.5 | 1.68 (0.56, 4.99) | 0.52 (0.19, 1.46) | 0.42 (0.17, 1.05) |
| 6 | 5.5 | 0.60 (0.26, 1.38) | 5.25 (1.14, 24.07) | 2.63 (1.03, 6.72) |
| 7 | 3.7 | 1.08 (0.56, 2.10) | 1.78 (0.68, 4.65) | 1.41 (0.39, 5.05) |
| 8 | 3.2 | 0.32 (0.11, 0.88) | 0.22 (0.05, 0.93) | 0.82 (0.42, 1.58) |
| 9 | 2.7 | 1.39 (0.58, 3.30) | 1.59 (0.54, 4.65) | 1.41 (0.72, 2.74) |
| 10 | 2.1 | 2.95 (1.19, 7.34) | 6.36 (1.77, 22.82) | 0.86 (0.43, 1.74) |
| 11 | 2.0 | 0.75 (0.28, 2.03) | 0.75 (0.22, 2.55) | 0.98 (0.45, 2.14) |

*Adjusted odds ratio (95% confidence interval)

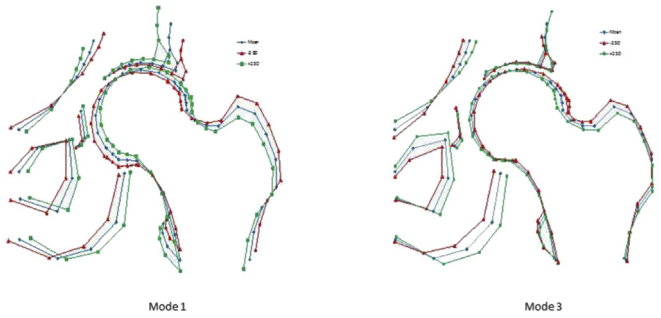


Figure. Modes associated with LLI outcomes (Mean=blue, -2 SD=red, +2 SD=green).

## 59
## MECHANO-REGULATION OF WNT-SIGNALLING IN ARTICULAR CARTILAGE

A. Al-Sabah, V. Duance, E. Blain. *Cardiff Univ., Cardiff, United Kingdom*

**Purpose:** Purpose: WNT signalling is one of the major regulators of cartilage development, differentiation and homeostasis. Recent human and animal studies have suggested that the dysregulation of WNT